NANO-HETEROEPITAXY STRESS AND STRAIN ANALYSIS: FROM MOLECULAR DYNAMIC SIMULATIONS TO CONTINUUM METHODS

A Thesis
Presented to
The Academic Faculty

by

Wei Ye

In Partial Fulfillment
of the Requirements for the Degree
Master in the
School of Mechanical Engineering

Georgia Institute of Technology
August 2010

NANO-HETEROEPITAXY STRESS AND STRAIN ANALYSIS: FROM MOLECULAR DYNAMIC SIMULATIONS TO CONTINUUM METHODS

Approved by:

Dr. Mohammed Cherkaoui, Advisor
School of Mechanical Engineering
Georgia Institute of Technology

Dr. Abdallah Ougazzaden, Co-advisor
School of Electrical and Computer Engineering
Georgia Institute of Technology

Dr. Ting Zhu
School of Mechanical Engineering
Georgia Institute of Technology

Date Approved: April 6, 2010

To my family and my friends

ACKNOWLEDGEMENTS

In this work, I need to devote my thanks to my advisor, Dr. Cherkaoui and my co-advisor, Dr. Ougazzaden first. Now I still remember that, when I came to Georgia-tech, Lorraine campus in the summer of 2008, both of them welcomed me to join this work group, and our work is indeed a close cooperation between the mechanical engineering lab, which I am currently in, and one ECE lab working on semiconductor and epitaxy. The former lab is about material designs by computing and modeling method under the direction of Dr. Cherkaoui, while the ECE lab can provide experimental support with the help of Dr. Ougazzaden. Therefore, I feel grateful to benefit from both side.

During the process of this work, I am fortunate to receive the help of many other people. For technical problems, especially at the beginning of doing molecular dynamic simulations, I was so frustrated there because I was totally a beginner at that time(so far, I still consider myself as a green-hand when thinking of the vast applications of this powerful tool). I honestly devote my thanks to Dr. Raulot who is not registered in Georgia-tech, Lorraine campus but works in the lab of University of Metz here in France. I thank him deeply for his enthusiasm and hours and hours discussions on simulations. Although we are using different simulation softwares and it really cause problems sometimes, his ideas about this field and principal explanations are quite useful for me.

I also want to thank the people I have been working with or studying with here in the city of Metz. Dr. Berbenni is also from a French institution and he always would like to share his ideas in our meeting. After this, I need to thank a group of people here that

have made my life in this campus colorful and enjoyful, such as Sadiq, Malek, Mathieu, Frances and many, many other people that I can't list our here.

At the end, I will alway thank my family members in my homeland. My grandma and parents were a litte sad when I chose the pursuit of studying abroad, but they understand me unconditionally. My brother is the one always encouraging me up and always giving his advices for me. Above all, I dedicate my deepest thanks and love to my family.

TABLE OF CONTENTS

LIST OF TABLES

LIST OF FIGURES

LIST OF SYMBOLS AND ABBREVIATIONS

C_{ijkl}	stiffness tensor
ε_{ij}	strain tensor
σ_{ij}	stress tensor
Γ	surface excess energy
Γ_0	Intrinsic surface/interface excess energy
$\Gamma^{(1)}$	Residual surface/interface stress
$\Gamma^{(2)}$	Surface/interface's in-plane elasticity
ε^s	In-plane deformation
C11	Stiffness tensor component of C_{1111}
C12	Stiffness tensor component of C_{1122}
ε_0	Natural strain due to lattice mismatch
ε^*	Lateral strain
l	Basal length of nanoisland
h	Height of nanoisland
w1	Bulk elastic energy of nanoisland
w2	Surface elastic energy of nanoisland
w	Total elastic energy of nanoisland

SUMMARY

For decades, epitaxy is used in nanotechnologies and semiconductor fabrications. So far, it's the only affordable method of high quality crystal growth for many semiconductor materials. Heterostructures developed from these make it possible to solve the considerably more general problem of controlling the fundamental parameters inside the semiconductor crystals and devices. Moreover, as one newly arising study and application branch of epitaxy, selective area growth (SAG) is widely used to fabricate materials of different thicknesses and composition on different regions of a single wafer. All of these new and promising fields have caught the interests and attentions of all the researchers around the world.

In this work, we will study the stress and strain analysis of epitaxy in nano-scale materials, in which we seek a methodology to bridge the gap between continuum mechanical models and incorporate surface excess energy effects, which can be obtained by molecular dynamical simulations. We will make a brief description of the elastic behavior of the bulk material, covering the concepts of stress, strain, elastic energy and especially, the elastic constants. After that, we explained in details about the definitions of surface/interface excess energy and their characteristic property tensors. For both elastic constants and surface excess energy, we will use molecular dynamic simulations to calculate them out, which is mainly about curve-fitting the parabola function between the total strain energy density and the strain.

After this, we analyzed the stress and strain state in nanoisland during the selective area growth of epitaxy. When the nanoisland is relaxed, the lattice structure becomes equilibrated, which means the total strain energy of system need to be minimized. Compared to other researcher's work, our model is based on continuum mechanics but also adopts the outcome from MD simulations. By combining these

microscopic informations and those macroscopic observable properties, such as bulk elastic constants, we can provide a novel way of analyzing the stress and strain profile in epitaxy. The most important idea behind this approach is that, whenever we can obtain the elastic constants and surface property tensors from MD simulations, we can follow the same methodology to analyse the stress and strain in any epitaxy process. This is the power of combining atomistic simulations and continuum method, which can take considerations of both the microscopic and macroscopic factors.

CHAPTER 1

INTRODUCTION

This chapter provides an introduction to the world-widely used epitaxy technology in fabricating nano-scale devices. Based on a review of the works from other scientists and researchers, we will present different approaches in epitaxy modeling, and then discuss the motivations and goals of our project. At the end of this chapter, we will give a brief description of our approach and the work that has been done.

The State-of-Arts of Epitaxy

It is impossible to imagine modern solid-state applications and devices nowadays without semiconductor heterostructures. Among those structures, quantum wells, wires, and dots are the subject of research of two-thirds of the semiconductor physics community. For decades, epitaxy is used in nanotechnologies and semiconductor fabrications. So far, it's the only affordable method of high quality crystal growth for many semiconductor materials, including technologically important materials as silicon-germanium, gallium nitride, gallium arsenide, indium phosphide and graphene.

In epitaxy, a monocrystalline film is deposited onto a monocrystalline substrate. If the materials are the same with each other, it's called homoepitaxy; otherwise it is called heteroepitaxy. Heterostructures developed from these make it possible to solve the considerably more general problem of controlling the fundamental parameters inside the semiconductor crystals and devices: band gaps, effective masses of the charge carriers and the mobilities, refractive indices, electron energy spectrum, etc[1].

Selective area growth (SAG) is a metalorganic chemical vapor deposition (MOCVD) technique widely used to fabricate materials of different thicknesses and composition on different regions of a single wafer. As growth precursors shower down on

the wafer, they do not react on the oxide and hence must diffuse to the exposed region for growth. The exposed regions in between the oxide pads accumulate more material compared to the regions that are further away from these pads. This is the key idea behind SAG.

Selective area growth has found wide ranging applications in optoelectronic integrated circuits, e.g., integrated electro-absorption modulated lasers[2], beam expanded lasers[3], and transceivers[4].

Motivations and Goals

In the past a few years, the modeling of epitaxy has been investigated by many researchers. During the epitaxy process, it involves complex and strongly coupled phenomena occurring at multiple length and time scales. Fast elementary processes such as migration of adsorbed molecules at the film surface, chemical reactions or atomic relaxation have characteristic times of 10^{-10} ~ 10^{-15}s and involve displacements of approximately 10^{-10} m. Numerous numerical models have been developed to simulate the process, but most of them have focused only on particular scales[5-7]. Recently, multiscale simulation has emerged as one of the most promising interdisciplinary field of investigation in Computational Materials Science. It is a promising route towards the prediction of the microstructure and properties of materials prepared by epitaxy.

In multiscale modeling, linking macroscale to micro- or atomic scale often turns out to be the primary focus. For years, continuum mechanics-based micromechanics theories have been used widely and successfully to model conventional polycrystalline and composite materials, because the material can be still considered as a continuum media to some extent. However, nanomaterials are characterized by their microstructures with their fine length scale, and therefore exhibit some new and important properties and behaviors. For instance, the surface area to volume ratio increases tremendously when the length scale of the material drops from metres to nanometres, thus it’s nessessary to take

consideration of surface or interfacial properties in modeling the properties and behavior of nanomaterials.

In our work, we studied the stress and strain analysis of heteroepitaxy in nano-scale materials, in which we seek a methodology to bridge the gap between continuum mechanical models and incorporate atomistic effects, surface excess energy in our case. Furthermore, to study the atomistic effects of nanomaterials, this resorts to molecular dynamical simulations, which enable us to understand and model the collective behavior of the atoms. By combining these microscopic informations and those macroscopic observable properties, such as bulk elastic constants, we can provide a novel way of analyzing the stress and strain profile in epitaxy.

CHAPTER 2

MOLECULAR DYNAMIC SIMULATIONS

Introduction to Different Simulations

Nowadays, simulation models can cover quite a broad area of research interests and also involves different scales of length and timestep[8]. Basically, in any simulation, first, a hierarchy of length and time scales is established within the physical ensemble. Second, the elementary objects (atoms, clusters, grains, etc.) handled on the various scales of interest are defined. Third, those physical processes which are irreducible and independent at a given length scale are identified. The processes and objects handled at a given scale usually represent 'averages' calculated at the immediately lower scale.

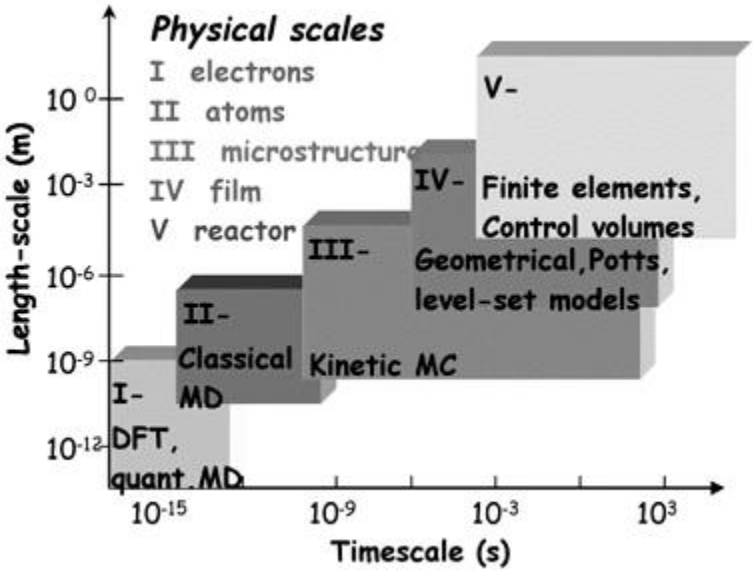

Figure 1: Simulation models in Materials Science and related length and time scales[8].

In Figure 1 above, it shows the characteristic length and time scales accessible to the main types of simulation models used in Materials Science. Ab initio methods such as

density functional theory (DFT) or Carr–Parrinello (CP) Molecular Dynamics[9] are capable of describing electronic interactions between a few hundreds of atoms, in static (DFT) or over extremely short time scales (10^{-13} s for CP). They are generally used to calculate transition state structures, surface reaction pathways, etc. Electronic interactions are represented by empirical potentials in classical Molecular Dynamics models[10], thus enabling the simulation of the real atomic motions in systems of typically 10^5 atoms over 10^{-9} s. Classical Monte Carlo models[11] can also be used to determine the equilibrium state of molecular systems of this size, but they do not provide accurate information on dynamics. Conversely, Kinetic Monte Carlo (KMC) models, which are generally lattice-based, are capable of simulating atomic motions in systems consisting of more than 10^6 atoms over typically 10^3 s[12]. KMC models do not provide a description of atomic interactions as accurate as MD models, but they have a unique potential of bridging atomic scale and microscopic scale in dynamic simulations. Finally, continuum models based on finite elements or finite volume methods are generally used to simulate transport phenomena inside the preparation chamber[13].

MD Simulations Tool: LAMMPS

LAMMPS[14] is a classical molecular dynamics code that models an ensemble of particles in a liquid, solid, or gaseous state. It can model atomic, polymeric, biological, metallic, granular, and coarse−grained systems using a variety of force fields and boundary conditions. It can model systems with only a few particles up to millions or billions. LAMMPS runs efficiently on single−processor desktop or laptop machines, but is designed for parallel computers. It will run on any parallel machine that compiles C++ and supports the MPI message−passing library. This includes distributed− or shared−memory parallel machines and Beowulf−style clusters. As a freely−available open−source code, most information can be checked on the LAMMPS WWW Site (http://lammps.sandia.gov).

In MD simulations or any other atomistic simulations, the interatomic potentials are at the heart of the simulations. In classical atomistic simulations, the atoms are represented by mass-points in space interacting through many-body interactions potential. The complex description of electrons dynamics is abandoned and an effective depiction is taken. In this picture, the interatomic interaction and internal degrees of freedom are completely defined by a set of parameters and functions which depend on the positions of the atoms in the system.

In our work, we compute pairwise interactions for metals and metal alloys using embedded−atom method (EAM) potentials[15]. In the EAM framework, the total energy of an atom is expressed as the sum of the contribution from the energy of two-body interactions and the embedding energy incorporating the complex nature of metallic cohesion. Among all of the interatomic potentials, the EAM method is a very efficient technique for modeling realistic descriptions of metallic cohesion. It is a semi-empirical approach that uses multi-atom potential for modeling the interatomic forces. In this scheme all atoms are treated in a unified way. The method is so called "embedded" because it views each atom individually as if it was embedded in a host lattice comprising all other atoms. It has the important benefit of keeping the computational scaling on the order of magnitude of N (if N is the number of particle composing the system) whereas more complex and thorough many-body potential scale on the order of magnitude N^3 (for instance, Density Functional Theory).

CHAPTER 3

DESCRIPTIONS OF BULK AND SURFACE PROPERTIES

This chapter will mainly recall the fundamental basics of continuum mechanics. In the description of the elastic behavior of the bulk material, we will cover the concepts of stress, strain, elastic energy and especially, the elastic constants. After that, we will spend more on explaining the properties of surfaces or interfaces. In that part, we will see the definitions of surface/interface excess energy and their characteristic property tensors.

Elastic Constants of Bulk Materials

In continuum mechanics, the elastic constants of crystal material is well defined. To keep consistent with the ideas of atomistic simulations later, here we introduce the elastic constants through the Taylor's expansion of the total strain energy density at the state of zero stress and strain[16].

$$E = \frac{1}{2} C_{ijkl}\, \varepsilon_{ij}\, \varepsilon_{kl} + \frac{1}{6} C_{ijklmn}\, \varepsilon_{ij}\, \varepsilon_{kl}\, \varepsilon_{mn} + \cdots$$

where ε_{ij} is the Lagrangian strain measured from the perfect lattice of an undeformed crystal of infinite extent, C_{ijkl} is a fourth order stiffness tensor consists of second order elastic constants, and C_{ijklmn} is a sixth order tensor consisting of the third order elastic constants of the solid. All are defined in the reference configuration, or the initial stress-free configuration. In our case, we will neglect the sixth order and higher order items.

The symmetric Piola-Kirchhoff stress is the gradient of the strain energy with respect to the strain.

$$\sigma_{ij} = \frac{\partial E}{\partial \varepsilon_{ij}} = C_{ijkl}\, \varepsilon_{kl}$$

In crystals, because of the symmetry of the structure systems, some components in the stiffness tensor C_{ijkl} will be null, and the most general anisotropic elastic solids require only 21 elastic constants. We can write the stiffness tensor in the following way.

$$C = \begin{bmatrix} C_{1111} & C_{1122} & C_{1133} & C_{1123} & C_{1113} & C_{1112} \\ C_{1122} & C_{2222} & C_{2233} & C_{2223} & C_{2213} & C_{1222} \\ C_{1133} & C_{2233} & C_{3333} & C_{2333} & C_{1333} & C_{1233} \\ C_{1123} & C_{2223} & C_{2333} & C_{2323} & C_{2313} & C_{1223} \\ C_{1113} & C_{2213} & C_{1333} & C_{2313} & C_{1313} & C_{1213} \\ C_{1112} & C_{1222} & C_{1233} & C_{1223} & C_{1213} & C_{1212} \end{bmatrix}$$

The indices of the notation above are quite cumbersome, so it's often in a simplified or contracted form.

$$C = \begin{bmatrix} C_{11} & C_{12} & C_{13} & C_{14} & C_{15} & C_{16} \\ C_{12} & C_{22} & C_{23} & C_{24} & C_{25} & C_{26} \\ C_{13} & C_{23} & C_{33} & C_{34} & C_{35} & C_{36} \\ C_{14} & C_{24} & C_{34} & C_{44} & C_{45} & C_{46} \\ C_{15} & C_{25} & C_{35} & C_{45} & C_{55} & C_{56} \\ C_{16} & C_{26} & C_{36} & C_{46} & C_{56} & C_{66} \end{bmatrix}$$

In this contracted form, C_{ij} is no longer the component of a second order tensor.

Considering some special materials, such as monoclinic, orthotropic or isotropic materials, they have planar or axial symmetry in their structure themselves, so the form can be even simplified more. In the next chapter, we will see the calculation of elastic constants for pure metals, for example, copper has FCC cubic lattice structure, and its stiffness tensor can be written as the following.

$$C = \begin{bmatrix} C_{11} & C_{12} & C_{12} & & & \\ C_{12} & C_{11} & C_{12} & & 0 & \\ C_{12} & C_{12} & C_{11} & & & \\ & & & C_{44} & 0 & 0 \\ & 0 & & 0 & C_{44} & 0 \\ & & & 0 & 0 & C_{44} \end{bmatrix}$$

Surface/Interface Excess Energy

Evolution of "Surface Energy" Concept

The initial idea of "surface energy" can date back to the year of 1928 when Gibbs first formulated the thermodynamics of a fluid interface through the use of interfacial free energy, which is a single dividing surface used to separate two homogeneous phases, and the interface contribution to the thermodynamic properties is defined as the excess over the values that would be obtained if the bulk phases retained their properties constant up to an imaginary surface (of zero thickness) separating the two phases. Gibbs showed that various combinations of the interfacial excess quantities can yield physically meaningful and experimentally measurable variables which are independent of the dividing surface position. By following Gibbs' work, Shuttleworth and many other researchers[14-16] extended this Gibbsian description of fluid-fluid interfaces to solid-solid interfaces and to associate a "surface stress" with the change of in interfacial energy upon deformation. From then on, instead of considering the surface excess energy as a constant quantity in all situations, researchers began to take the surface excess energy as a function of the surface strain, which is only due to the in-plane deformation. For example, Shama[17] has used the Shuttleworth equation for solid-solid interfaces such as grain boundaries. On the other hand, although there are many similarities between a free surface and an interface in elastic solid, in the early 80s, Andreev and Kosevich[18] already noticed that there is one key difference between them, namely, in addition to in-plane deformation, an interface may be subjected to transverse (normal to the interface) stress. Such transverse stress and the corresponding transverse deformation also contribute to the interfacial excess, but they did not give an expression of the contribution from the transverse stress. Recently, Dingreville[19] provided a comprehensive way of determining the interfacial excess energy by taking consideration of both in-plane deformation and the effects of

transverse stress. Later, Dingreville and Qu[20] successfully applied this approach to estimate interface elastic properties with a semi-analytical method of calculation.

Definition of Surface Excess Energy

Before we come to the definition of surface excess energy, it's remarkable to mention that there are typically two ways in which the properties of the surface can be defined and introduced. The first one is an "interphase" model, and the system is considered to be one in which there are three phases present – the two bulk phases and an inter-phase; the boundaries of the inter-phase are somewhat arbitrary and are usually chosen to be at locations at which the properties are no longer varying significantly with position. The inter-phase then has a finite volume and may be assigned thermodynamic properties in the normal way[21]. In the second approach where a single dividing surface is used to separate the two homogeneous phases, the interface contribution to the thermodynamic properties is defined as the excess over the values that would obtain if the bulk phases retained their properties constant up to an imaginary surface (of zero thickness) separating the two phases. In this work, we will take the second definition.

The surface free (excess) energy of a near surface atom, E_n is defined by the difference between its total energy and that of an atom deep in the interior of a large bicrystal. Clearly, E_n depends on the location of the atom.

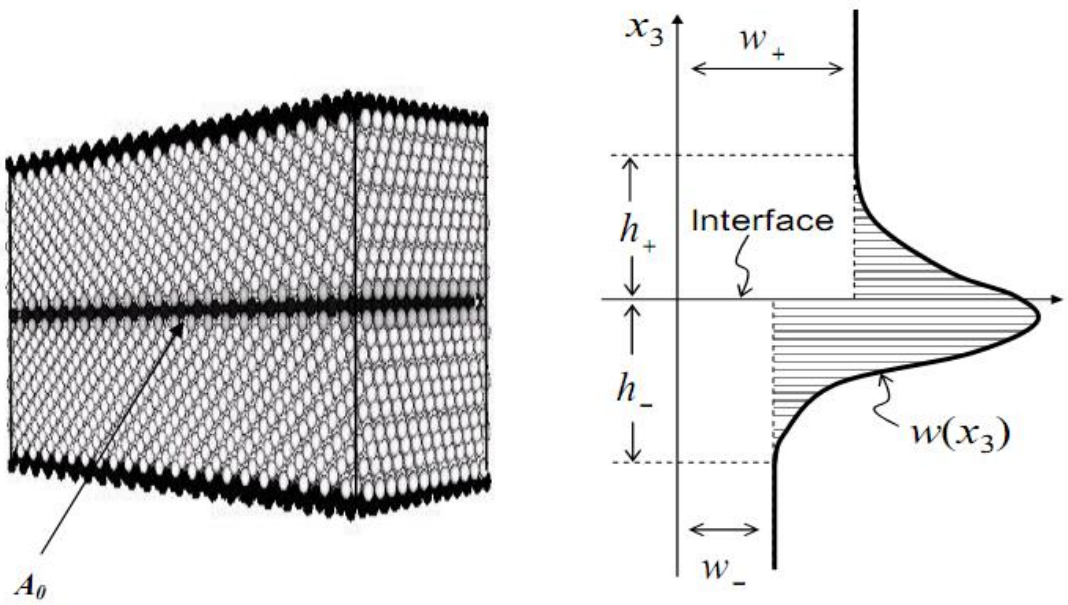

(a) (b)

Figure 2: Demonstration for bicrystal interface[19]

(a) Flat interface of a bimaterial, (b) Interface excess energy as a function of the distance away from the interface

For the bicrystal interface shown in Figure 2(a), the x3-dependence of E_n is schematically shown in Figure 2(b), i.e., it reaches its maximum value on the interface and tends to zero deep into the crystal. If there are N atoms surrounding an area A in the deformed configuration, the Gibbs surface excess energy density is defined as the following.

$$\Gamma = \frac{1}{A}\sum_{i=1}^{N} E_i$$

From the work of Dingreville[19], this surface excess energy is linked to the surface stress and surface strain by introducing some surface property tensors. It then follows that the interfacial excess energy can be re-rewritten as

$$\Gamma = \Gamma_0 + \Gamma^{(1)}:\varepsilon^s + \frac{1}{2}\varepsilon^s:\Gamma^{(2)}:\varepsilon^s + \frac{1}{2}\sigma_+^t:\Lambda^{(2),+}:\sigma_+^t + \frac{1}{2}\sigma_-^t:\Lambda^{(2),-}:\sigma_-^t$$

with ε^s and σ^t are, respectively, the in-plane strain and transverse stress tensors, and other tensorial terms are intrinsic properties of the interface. It is obvious that if no stress or strain is applied, the surface excess energy form is reduced to only the first item, Γ_0, which becomes a constant quantity, and this is consistent to the definition originally introduced to fluid surfaces. However, when stress or strain is applied, the surface excess energy is no longer an intrinsic material property, but also depends on the applied load. terms. The second term, $\Gamma^{(1)}$, is a two-dimensional second order tensor representing the internal excess stress of the interface. It is the part of interfacial stress that exists when the surface strain and transverse stress are absent. The third term, $\Gamma^{(2)}$, is related to the two-dimensional fourth order tensor that represents the interface's in-plane elasticity. Finally, $\Lambda^{(2)}$ represents the transverse compliance of the interface which can be taken as kind of the interfacial transverse compliant tensor.

On contrast of bicrystal interfaces, if we only consider a free surface with only one material, then there is no transverse effect involved and the free surface excess energy can be truncated as,

$$\Gamma = \Gamma_0 + \Gamma^{(1)}: \varepsilon^s + \frac{1}{2}\varepsilon^s: \Gamma^{(2)}: \varepsilon^s$$

The surface property tensors, Γ_0, $\Gamma^{(1)}$, $\Gamma^{(2)}$ are intrinsic properties of the free surface. In the following chapters, they can be calculated for a given material with known interatomic potentials by molecular dynamic simulations. Once these tensors are known, the elastic behavior of the surface is fully characterized.

CHAPTER 4

RESULTS FROM MD SIMULATIONS

This chapter will focus on the calculation of elastic constants and surface excess energy by MD simulations in LAMMPS. For each part, we will present the calculation framework and methodology first, and then provide the results for discussion.

Calculations of Elastic Constants

Recall the formulation from the chapter above, for cubic pure metals such as Cu, Al, etc, the stiffness tensor can be written as the following.

$$C = \begin{bmatrix} C_{11} & C_{12} & C_{12} & & & \\ C_{12} & C_{11} & C_{12} & & 0 & \\ C_{12} & C_{12} & C_{11} & & & \\ & & & C_{44} & 0 & 0 \\ & 0 & & 0 & C_{44} & 0 \\ & & & 0 & 0 & C_{44} \end{bmatrix}$$

The total strain energy density at the state of zero stress and strain is as following.

$$E = \frac{1}{2} C_{ijkl}\, \varepsilon_{ij}\, \varepsilon_{kl}$$

The calculation procedures of the three elastic constants are quite similar. The principle is based on curve-fitting the parabola function between the total strain energy density and the strain.

To simulate an infinite crystal, we constructed a rectangular cell and used periodic boundary conditions in all directions to mimic a crystal of infinite extend. A typical calculation cell contains 500 atoms. A bigger calculation sample is not necessary since the dimension of the calculation box are chosen to be at least twice as big as the cut-off distance of the interatomic potential.

For calculations, we have performed a strain meshing of the calculation cell with strains in the three directions ranging from -1% to 1% and incremented by ±0.01% strain

steps. The calculation cell is stretched by independently varying the lattice constants along the three directions. This state corresponds to the energy state of the cell in the strain space. The procedure yields to a strain mesh of the total strain energy of the sample with respect to the reference configuration. The general steps of the calculation can be outlined as follows:

(a) Create the initial assembly using the given material properties (atomic weight, lattice spacing, EAM potential, crystallographic orientation, etc…).

(b) Apply a small strain field to the assembly.

(c) Compute the energy density corresponding to this given strain field.

(d) Increase the magnitude of strain and repeat steps (b) and (c).

After repeating steps (b) – (d) a sufficient number of times, we obtain a mesh strain energy density of as a function of the strain. A numerical interpolation of the energy density was performed to evaluate the elastic constants.

Elastic Constant C11

By applying strain as $\varepsilon_{11} = \varepsilon$ and other strain components as zero(see Figure 3), The total strain energy density is simply as $E = \frac{1}{2} C_{11} \varepsilon^2$.

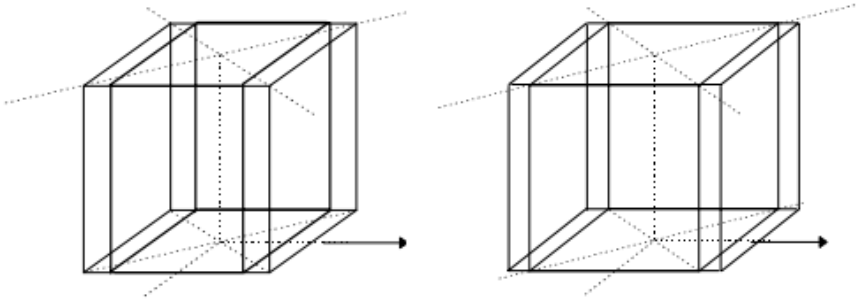

(a) (b)

Figure 3: Deformation applied to the crystal Cu for calculation of C11

(a. Before deformation; b. After deformation)

The interpolation result of the energy density v.s strain is shown in Figure 4 below, and the value obtained is C11 = 173.2 GPa.

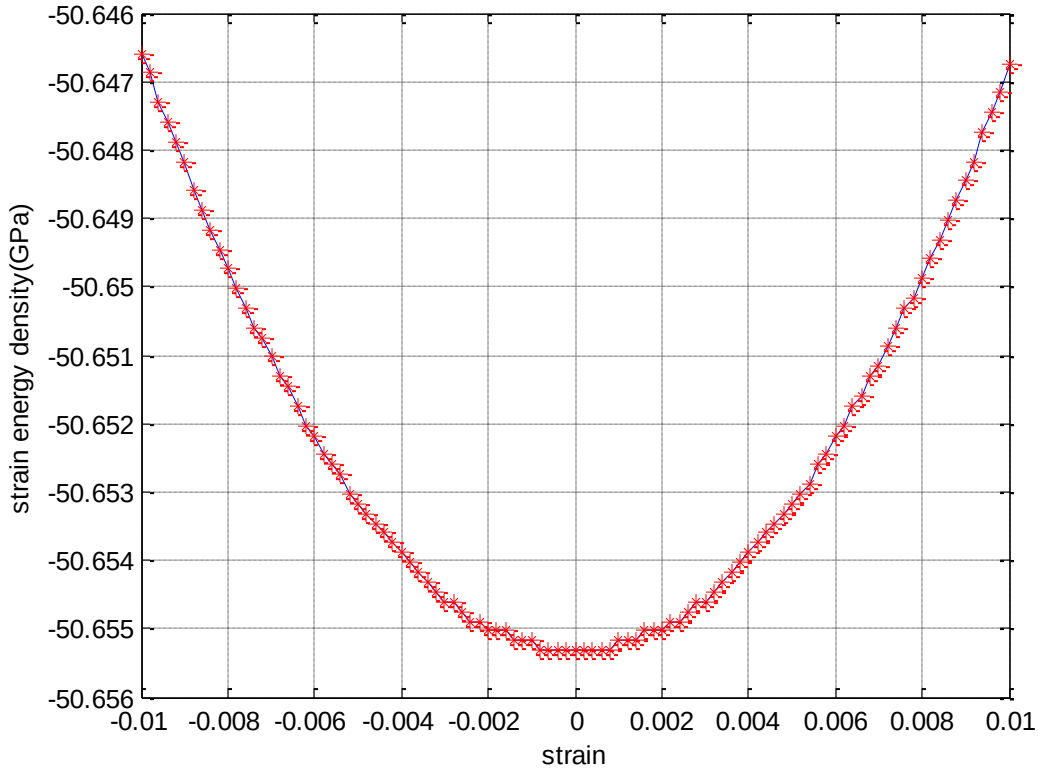

Figure 4: Interpolation result of C11 of copper

Elastic Constant C12

By applying strain as $\varepsilon_{11} = -\varepsilon_{22} = \varepsilon$ and other strain components as zero(see Figure 5), The total strain energy density is simply as $E = (C_{11} - C_{12})\varepsilon^2$.

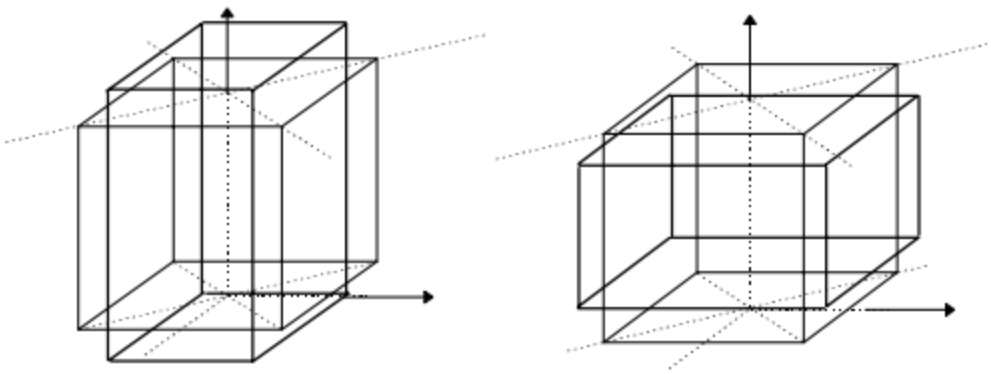

(a) (b)

Figure 5: Deformation applied to the crystal Cu for calculation of C12

(a) Before deformation; (b) After deformation

The interpolation result of the energy density v.s strain is shown in Figure 6 below, and the value obtained is C12 = 129.2 GPa.

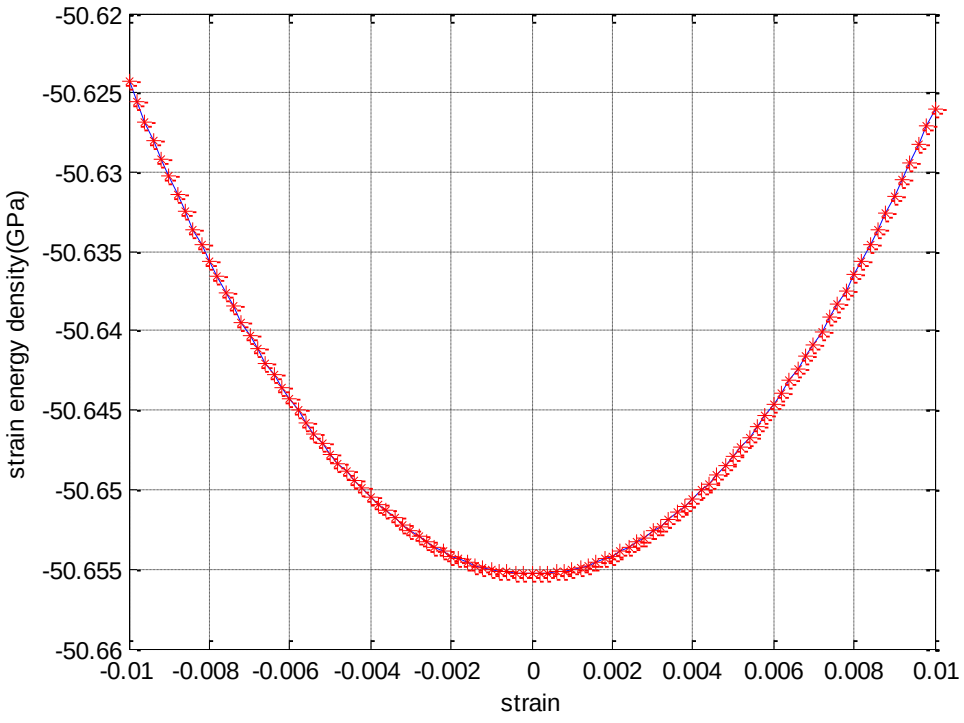

Figure 6: Interpolation result of C12 of copper

This methodology for calculation of elastic constants is quite efficient and satisfactory. As long as a proper interatomic potential of the material is provided, its elastic constants can just be obtained by following this standard procedure. In our work, we also test this with other materials and compare our results to those literatures. The final results are listed in the table below.

Table 1: Results of elastic constants by MD simulations(unit: GPa)

	Cu	Au	Pd	Pt
C11	167.1[19]/166.1[22] 173.2	183.1[19]/192.9[22] 189.1	198.3[19]/224.9	331.7[19]/313.0
C12	124.0[19]/119.9[22] 129.2	158.7[19]/163.8[22] 164.8	170.4[19]/191.9	294.2[19]/283.1

Calculations of Surface Excess Energy

The calculation procedures of the surface excess energy are quite similar. The principle is based on curve-fitting the parabola function between the total surface strain energy density and the strain. In our calculations, we have performed a strain meshing of the calculation cell with strains in the two planar directions ranging from -1% to 1% and incremented by ±0.01% strain steps. Periodic boundary conditions are used in the two planar directions with free surfaces in the vertical direction to mimic an infinite plane. The atomic interaction is prescribed through the EAM potential. By varying the number of layers of atoms in the vertical direction we can represent thin films of different thicknesses. The slab thickness must be chosen to be thick enough to avoid interaction between the two surfaces. The film is stretched by independently varying the lattice constants along the two planar directions, while atoms in the third direction can fully relax. Prior to any deformation, the first step of the calculation is to determine the self equilibrium state of the films. This state corresponds to the lowest energy state of the film in the strain space. The self equilibrium state serves as a reference configuration for the

crystal. The procedure just described yields to a mesh of the total strain energy of the sample with respect to the reference configuration. The surface free energy of a near surface atom is obtained by taking the difference between its total energy and that of an atom deep in the interior of a large crystal. The procedure described above can be outlined in the following steps:

(a) Create the initial assembly using the given material properties (atomic weight, lattice spacing, EAM potential, crystallographic orientation, etc.).

(b) Equilibrate the assembly to find the self equilibrium state.

(c) Apply a small strain field to the assembly and re-equilibrate.

(d) Compute the surface energy density corresponding to this given strain field.

(e) Increase the magnitude of strain and repeat steps (c) and (d).

After repeating steps (c) – (d) a sufficient number of times, we obtain a mesh of surface energy density as a function of surface strains. Through curve fitting, the coefficients of the surface property tensors, Γ_0, $\Gamma^{(1)}$, $\Gamma^{(2)}$ can be determined.

We first carried out this calculation for copper concerning (100) surface. Like the strategy of calculating elastic constants, the curve-fitting method is divided into two parts. By applying strain as $\varepsilon_{11} = \varepsilon$ and other strain components as zero, The total surface strain energy density is simply as,

$$\Gamma = \Gamma_0 + \Gamma_{11}^{(1)}\varepsilon + \frac{1}{2}\Gamma_{1111}^{(2)}\varepsilon^2$$

By applying strain as $\varepsilon_{11} = \varepsilon_{22} = \varepsilon$ and other strain components as zero, The total surface strain energy density is simply as

$$\Gamma = \Gamma_0 + (\Gamma_{11}^{(1)} + \Gamma_{22}^{(1)})\varepsilon + (\Gamma_{1111}^{(2)} + \Gamma_{1122}^{(2)})\varepsilon^2$$

Notice that in both interpolations, Γ_0 will be calculated. In this case, we also checked that the twice obtained values of Γ_0 here are the same. However, in our results listed in Table 2 below, the values of the second order tensor, $\Gamma^{(1)}$, deviates too much from other literature data.

Table 2: Results of surface tensors by MD simulations for Cu(100) surface(unit: J/m^2)

Γ_0	$\Gamma_{11}^{(1)}$	$\Gamma_{1111}^{(2)}$	$\Gamma_{1122}^{(2)}$
$1.288^{[19]}/1.28^{[23]}$	$1.396^{[19]}/1.38^{[24]}$	$-0.712^{[19]}$	$5.914^{[19]}$
1.3584	0.1118	-0.8328	5.3020

We also carried out the same calculation for (110) surface of copper, and similar discrepancy happened again for the values of the second order tensor(see Table 3).

Table 3: Results of surface tensors by MD simulations for Cu(110) surface(unit: J/m^2)

Γ_0	$\Gamma_{11}^{(1)}$	$\Gamma_{22}^{(1)}$	$\Gamma_{1111}^{(2)}$	$\Gamma_{2222}^{(2)}$	$\Gamma_{1122}^{(2)}$
$1.413^{[19]}$ /$1.40^{[23]}$ 1.4896	$-1.126^{[19]}/0.957^{[25]}$ 0.2889	$-0.993^{[19]}/0.957^{[25]}$ 0.4436	$-7.798^{[19]}$ -11.8204	$-2.263^{[19]}$ -3.0120	$-3.600^{[19]}$ -0.2657

Since part of the results turn out to be not so satisfactory, in the next chapter we will directly use the data from other literatures for further calculations.

CHAPTER 5

COMBINE MD SIMULATIONS AND CONTINUUM METHOD

This chapter is oriented to an example of selective area growth(SAG) strain analysis of nanoislands. We will first show the framework of formulating the problem by continuum mechanical models and incorporate atomistic effects, surface excess energy in our case. At the end we can compare the differences of choosing different surface excess energy formulations, and then we make a conclusion of our methodology of combining MD simulations and continuum method in stress and strain analysis in the applications of nanoepitaxy.

Nanoisland Strain Analysis in SAG

Traditional semiconductor epitaxial growth using planar, monolithic substrates has progressed from homoepitaxy to lattice-matched heteroepitaxy and recently to pseudomorphic, lattice-mismatched systems where small amounts of strain are accommodated in very thin films. In cases where a large lattice mismatch is unavoidable (e.g., GaN), then selective nucleation followed by lateral epitaxial overgrowth has also been shown to be successful in limiting the effects of mismatch defects by localizing them to inactive regions of the wafer[26].

Nanoheteroepitaxy exploits state-of-the-art lithography to pattern a substrate surface with nanoscale features (10–100 nm) prior to growth. Selective epitaxial growth is then performed and the epilayer nucleates as an array of nanoscale islands. The additional stress relief mechanisms available to nanoscale islands as compared to a conventional planar epilayer are illustrated in Figure 7. In a conventional planar structure the epilayer can only deform vertically (a) to relieve mismatch stress. In contrast, a nanoheteroepitaxy ‘‘island’’ consisting of a patterned substrate (lower part) and a

selectively grown epilayer (upper part), can deform vertically (a) and laterally (b). Thus the mismatch strain is distributed in three dimensions. In addition, the partitioning of strain between the epilayer and the substrate that occurs in nanoheteroepitaxy, will further reduce the amount of strain in the epilayer.

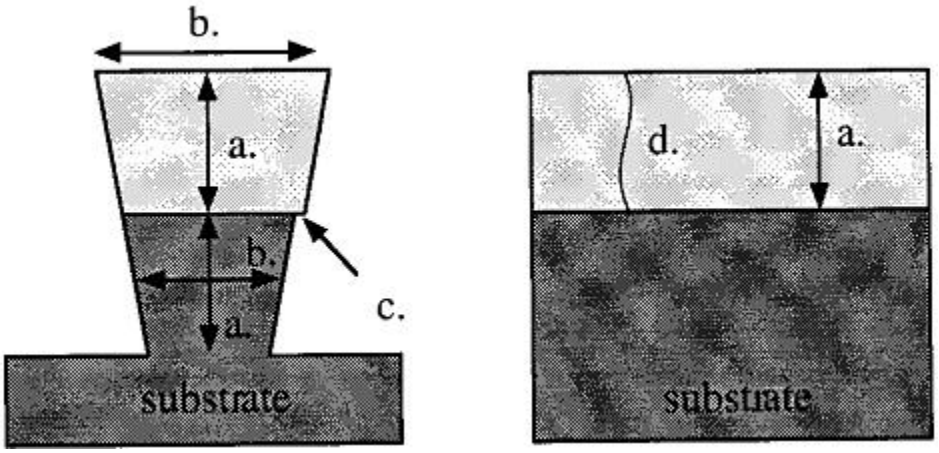

(a) (b)

Figure 7: Mismatch stress relief mechanisms comparasion

(a)nanoheteroepitaxy islands; (b)conventional planar heteroepitaxy sample.

When there is a misfit, the epitaxial contact of two crystals A and B can either be coherent or not coherent. The coherent epitaxial systems where the lattice planes in contact are in perfect registry over a large domain of intensive parameters (temperature, pressure, chemical potentials, etc.). During deposition, a transition from this perfect registry to a partial one occurs at some critical thickness[27], where the introduction of interfacial dislocations takes place. In this way the deposit abruptly releases strain energy by plasticity. On the contrary, non-coherent epitaxies are recognized when their contact lattice planes are out of registry. The periodicities of both lattice planes remain incommensurate. The atoms on both sides

of the interface glide[28] or rotate[29] slightly but continuously, so that the residual strain in the deposit decreases[30][31] without introduction of dislocations.

In Figure 8, if one cuts in A a piece (a) and accommodates it on the (001) substrate, the in-plane parameter a_0 has to be brought to b_0 (b), which means this piece has to be biaxially homogeneously strained. However, this constrained epitaxial system (b) is not in its elastic equilibrium state and then has to relax (c). Owing to surface stress, the piece of matter has a crystallographic parameter different from a_0.

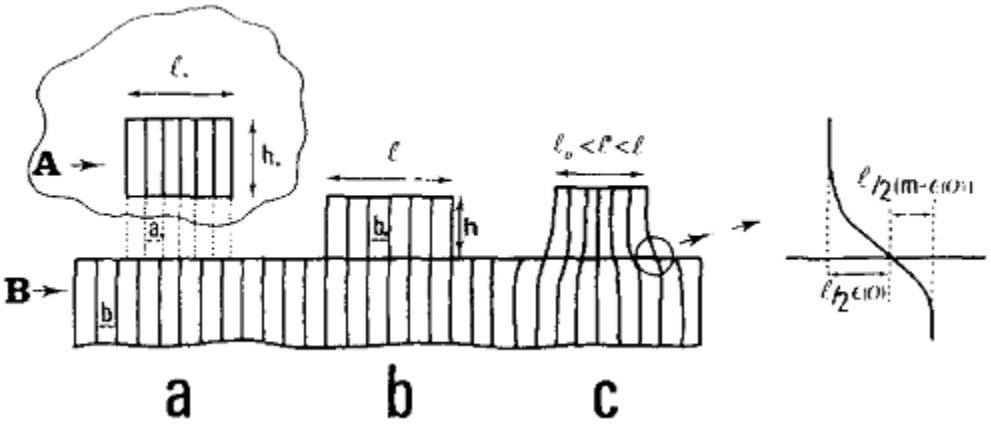

Figure 8: Demonstration of nanoisland under relaxation

(a) A 3D crystal A is cut in an infinite crystal; (b) Nanoisland in pseudomorphism with the substrate B by an homogeneous strain; (c) Nanoisland relaxes by dragging the substrate B.

In an epitaxial system, the conventional strain due to lattice misfit is defined as(crystallographic parameters a_0 and b_0 in materials A and B) :

$$\varepsilon_0 = \frac{b_0 - a_0}{a_0}$$

By comparision, the actual strain after relaxation becomes

$$\varepsilon = \varepsilon_0 - \varepsilon^*$$

where ε^* is called lateral strain[32]. ε^* is related to relaxation effect and it is especially significant when the length scale of the nanoisland goes down to nano scale.

To analyse the strain in such a nanoisland, we use macroscopic elastic constants up to monolayer sizes, which is now considered acceptable[33]. To introduce nano size effects properly we also consider surface stress, which means we consider surface stress. The knowledge we gain makes sense for islands, except for near-corner effects.

After the nanoisland is relaxed, the lattice structure becomes equilibrated, which means the total strain energy of system need to be minimized. Our framework of analysing the nanoisland begins with writing the system's strain energy in two parts:

(1)Bulk elastic energy contribution: according to continuum mechanics, the strain energy of a volume V is given as,

$$\mathrm{w1} = \int \left(\frac{1}{2} C_{ijkl}\, \varepsilon_{ij}\, \varepsilon_{kl}\right) dV$$

(2)Surface energy contribution: Γ is the surface energy density

$$\mathrm{w2} = \int \Gamma dV$$

The total strain energy of a volume V is the sum of the two contributions above:

$$w = \int (\frac{1}{2} C_{ijkl}\, \varepsilon_{ij}\, \varepsilon_{kl}) dV + \int \Gamma dV$$

Therefore, we obtain a relationship between the total strain energy and the strain state. Following the principle of minimizing the strain energy of equilibrium, we take the partial derivative of expression above and then obtain the equations to determine the strain state.

$$\frac{\partial w}{\partial \varepsilon_{ij}} = 0$$

In practical epitaxy applications, the strain distribution could be quite complex, which may vary for each point. On the other hand, considering the possibilities of all

kinds of nanoisland shapes in epitaxy, the surface energy term could be extremely complicated. In the work of R. Kern[32], they have provided analytical solution with the assumption of a very simplified case, in which the nanoisland is a rectangular shape with basis length of lx, ly ($lx = ly = l$), and height of lz ($lz = h$). They also considers the nanoisland as an isotropic material with Yong's modulus of E and Poission's ratio of v. Moreover, they assumed the nanoisland is subjected to a homogeneous triaxial strain and simplified constant surface stress of s_A (bottom and top faces) and $s_A^{'}$ (four lateral faces), which means all the surfaces are free surface since all the surface stress is only related to material A.

$$\varepsilon_{11}^{*} = \varepsilon_{22}^{*} = -\frac{1-v}{E}\left(\frac{2s_A}{h} + \frac{2s_A^{'}}{l}\frac{1-3v}{1-v}\right)$$

$$\varepsilon_{33}^{*} = -\frac{1-v}{E}\left(\frac{4s_A^{'}}{l} - \frac{2s_A}{h}\frac{2v}{1-v}\right)$$

The derivation of the formula is given in details in the work of R. Kern[32]. In their analysis, the lateral strain could be as great as 10^{-2} for films of only some atomic layers thick or islands of nanometric sizes.

Formulations of the Lateral Strain

In our work, we will also limit ourselves to triaxial strain case of elasticity and consider the same geometry shape of copper nanoisland with basis length of lx, ly ($lx = ly = l$), and height of lz ($lz = h$). By comparision, we will take the elastic constants from the calculation of MD simulations in chapter 4, and we consider all the six surfaces as free surfaces with surface energy density of Γ, where Γ is no longer a simple constant term but denoted by the surface excess energy as a function of strain state and those surface property tensors. In this way, the most important idea behind this approach is that, whenever we can obtain the elastic constants and surface property tensors from MD simulations, we can follow the same methodology to analyse the stress and strain in any epitaxy process, and quite a refined result can be obtained. This is the power of

combining atomistic simulations and continuum method, which can take considerations of both the microscopic and macroscopic factors.

The parameters of the problem are listed as following,

(a) Geometry of Cu nanoisland: l, h

(b) Elastic constants of Cu: C11, C12

(c) Surface property tensors: Γ_0, $\Gamma^{(1)}$, $\Gamma^{(2)}$

Following similar procedure, we write the system's strain energy in two parts: (1)Bulk elastic energy contribution: The strain energy of a volume V is given as,

$$w_1 = \frac{1}{2} l^2 h[C_{11}(\varepsilon_{11}^2 + \varepsilon_{22}^2 + \varepsilon_{33}^2) + C_{12}(\varepsilon_{11}\varepsilon_{22} + \varepsilon_{22}\varepsilon_{33} + \varepsilon_{33}\varepsilon_{11})]$$

(2)Surface energy contribution:

Bottom and top surface

$$s1 = 2l^2[\Gamma_0 + \Gamma_{11}^{(1)}(\varepsilon_{11} + \varepsilon_{22}) + \frac{1}{2}\Gamma_{1111}^{(2)}(\varepsilon_{11}^2 + \varepsilon_{22}^2) + \frac{1}{2}\Gamma_{1122}^{(2)}\varepsilon_{11}\varepsilon_{22}$$

Front and back surface

$$s2 = 2lh[\Gamma_0 + \Gamma_{11}^{(1)}(\varepsilon_{11} + \varepsilon_{33}) + \frac{1}{2}\Gamma_{1111}^{(2)}(\varepsilon_{11}^2 + \varepsilon_{33}^2) + \frac{1}{2}\Gamma_{1122}^{(2)}\varepsilon_{11}\varepsilon_{33}$$

Left and right surface

$$s3 = 2lh[\Gamma_0 + \Gamma_{11}^{(1)}(\varepsilon_{22} + \varepsilon_{33}) + \frac{1}{2}\Gamma_{1111}^{(2)}(\varepsilon_{22}^2 + \varepsilon_{33}^2) + \frac{1}{2}\Gamma_{1122}^{(2)}\varepsilon_{22}\varepsilon_{33}$$

Surface energy contribution is,

$$w2 = s1 + s2 + s3$$

The total strain energy of a volume V is the sum of the two contributions above:

$$w = \mathrm{w1} + \mathrm{w2}$$

Apply energy minimization

$$\frac{\partial w}{\partial \varepsilon_{ii}} = 0, \mathrm{i} = 1,2,3$$

We get the result for the strain state

$$\varepsilon_{11}^{*} = \varepsilon_{22}^{*} = -\left[4\Gamma_{11}^{(1)}\left(l^2C_{11} + lhC_{11} - lhC_{12} + 4l\Gamma_{1111}^{(2)} + 4h\Gamma_{1111}^{(2)} - 2h\Gamma_{1122}^{(2)}\right)\right]$$
$$/[2l^2hC_{11}^2 + l^2hC_{11}C_{12} - l^2hC_{12}^2 + 4l^2C_{11}\Gamma_{1111}^{(2)} + 2l^2C_{11}\Gamma_{1122}^{(2)}$$
$$+ 12lhC_{11}\Gamma_{1111}^{(2)} + 4lhC_{12}\Gamma_{1111}^{(2)} - 4lhC_{12}\Gamma_{1122}^{(2)} + 8l\Gamma_{1111}^{(2)}\Gamma_{1122}^{(2)}$$
$$+ 16l(\Gamma_{1111}^{(2)})^2 - 16h(\Gamma_{1111}^{(2)})^2 - 4h(\Gamma_{1122}^{(2)})^2]$$

$$\varepsilon_{33}^{*} = \left[4\Gamma_{11}^{(1)}\left(l^2C_{12} - 2lhC_{11} - 4l\Gamma_{1111}^{(2)} + 2h\Gamma_{1122}^{(2)}\right)\right]/[2l^2hC_{11}^2 + l^2hC_{11}C_{12} - l^2hC_{12}^2 +$$
$$4l^2C_{11}\Gamma_{1111}^{(2)} + 2l^2C_{11}\Gamma_{1122}^{(2)} + 12lhC_{11}\Gamma_{1111}^{(2)} + 4lhC_{12}\Gamma_{1111}^{(2)} - 4lhC_{12}\Gamma_{1122}^{(2)} +$$
$$8l\Gamma_{1111}^{(2)}\Gamma_{1122}^{(2)} + 16l(\Gamma_{1111}^{(2)})^2 - 16h(\Gamma_{1111}^{(2)})^2 - 4h(\Gamma_{1122}^{(2)})^2]$$

From these complex expressions, it's hard to tell the meaning behind them. In the following, we will discuss this result with respect to the lateral strain in two ways:

(1) Nano length scale effect;

(2) Surface excess energy effect.

Results and Discussions

From the results of MD simulations for copper in chapter 4, we already have C11=173.2GPa, C12=129.2GPa, $\Gamma_{11}^{(1)} = 1.38J/m^2$, $\Gamma_{1111}^{(2)} = -0.712J/m^2$, $\Gamma_{1122}^{(2)} = 5.914J/m^2$. These quantities will be used in the following calculations.

In SAG, the nanoisland size and shape can usually be decided manually because the epitaxy growth is carried out on the pre-patterned substrates. Therefore, it is nessessary to figure out how the length scale of the nanoisland will effect the lateral strain, and then will determine the final real strain. In our work, there are two dimension parameters involved for rectangular nanoisland: basis length of l, and height of h.

Effect of Dimension

Hold h=10nm as constant, l expands from 1~100 nm. The change of the lateral strain with dimension l is shown in Figure 9.

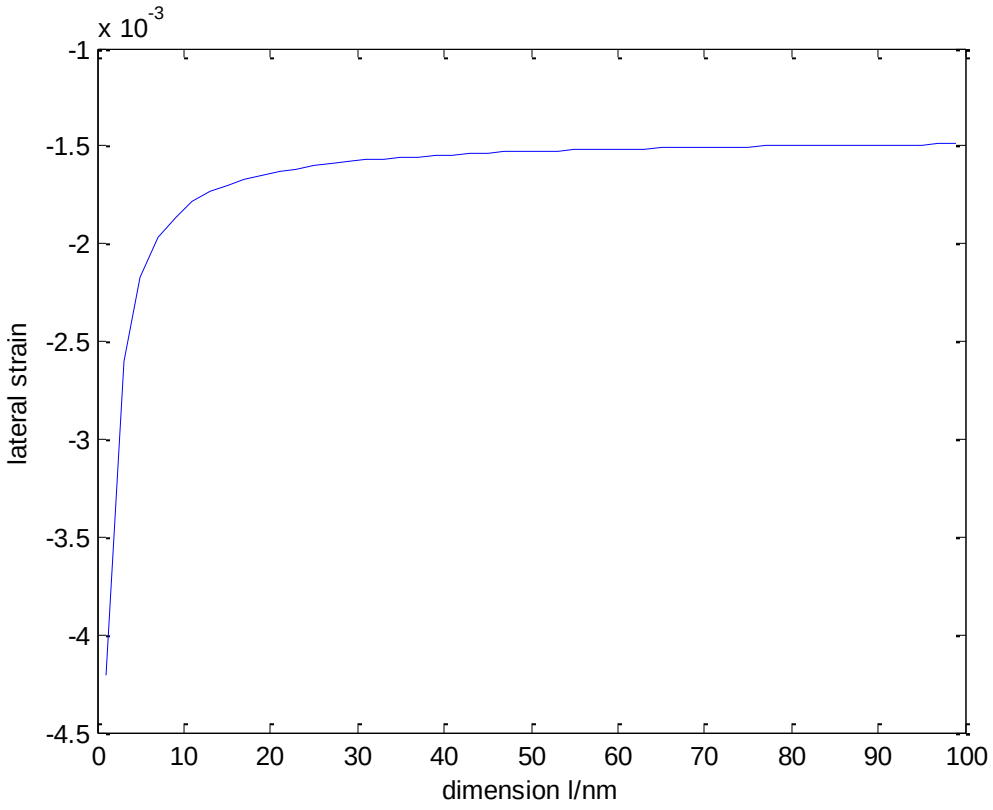

Figure 9: The change of the lateral strain with dimension l for dimension effect

Hold l=10nm as constant, h expands from 1~100 nm. The change of the lateral strain with dimension h is shown in Figure 10.

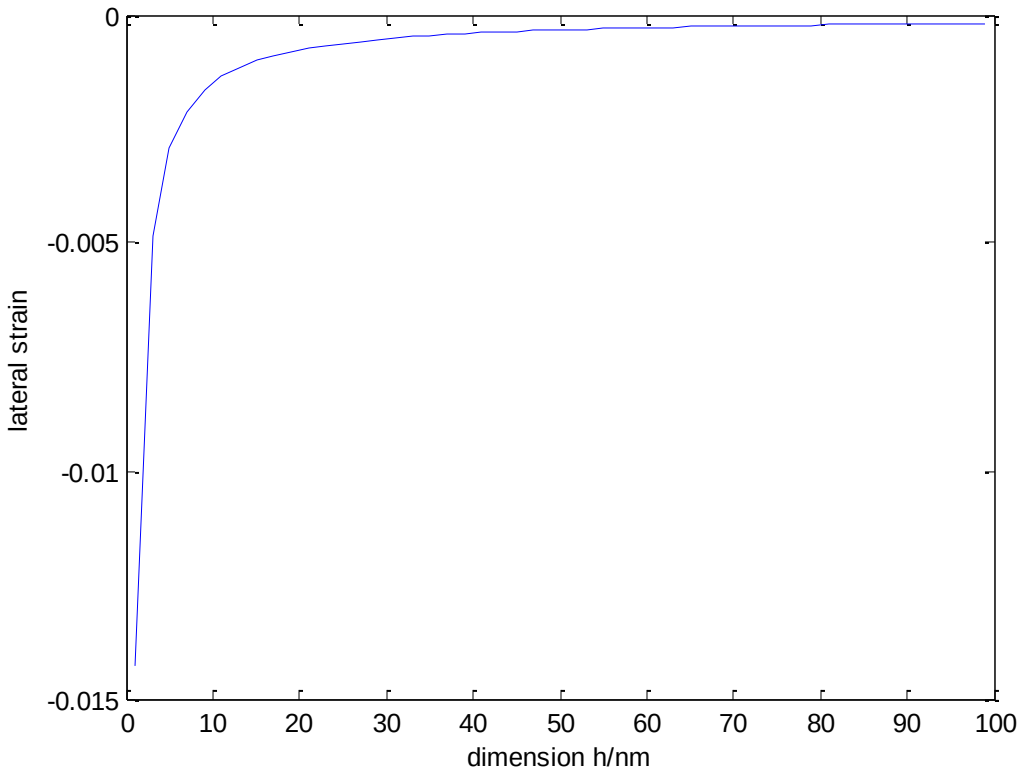

Figure 10: The change of the lateral strain with dimension h for dimension effect

From Figure 9 and 10, we can clearly observe the length scale of the nanoisland will effect the lateral strain significantly when it goes below 30nm. Another remarkable thing to mention here is that, from the magnitude of the absolute values of the lateral strain, the dimension h demonstrates a more important influence. This could be corresponded to the epitaxy experimental result. Because the material deposited later rests on top, the misfit is already compensated by the material below compared to the situation just near the interface. In this case, when the nanoisland is higher, averagely the strain energy density drops, so the lateral strain also drops.

Effect of Surface Excess Energy

Here we can investigate it in three cases:

(1) Consider no surface excess energy effects, which means Γ_0, $\Gamma^{(1)}$, $\Gamma^{(2)}$ are all zero, from the formulas above, it's obvious all lateral strain will be zero. This is a trivial check in our case.

(2) Consider only constant "surface stress" effects, which means Γ_0, $\Gamma^{(1)}$ are non-zero but $\Gamma^{(2)}$ is zero, our formulas reduce to the same result obtained by R. Kern[32].

(3) Consider non-constant "surface stress" effects, which means not only Γ_0, $\Gamma^{(1)}$ are non-zero but also $\Gamma^{(2)}$ is non-zero. In this case, we can compare the influence of $\Gamma^{(2)}$ term on the lateral strain with the result of (2).

In the third case, hold l=10nm as constant, h expands from 1~100 nm. The change of the lateral strain with dimension h is shown in Figure 11. Clearly the two curves almost overlap with each other.

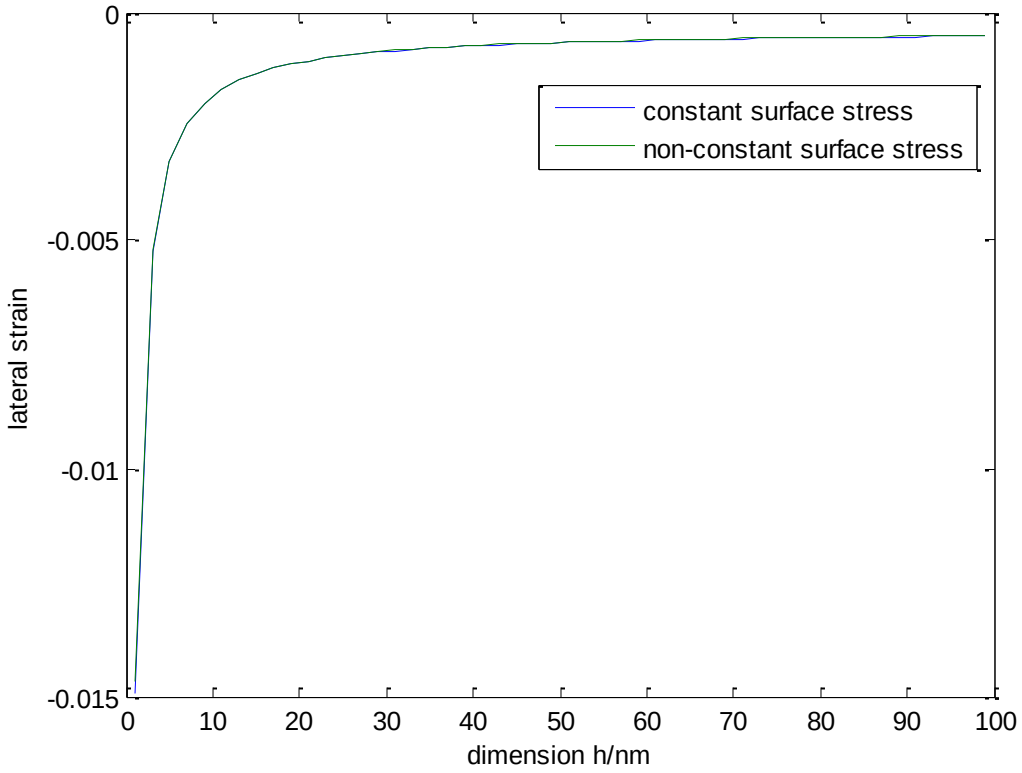

Figure 11: The change of the lateral strain with dimension h for surface effect(l=10nm)

Decrease dimension l little by little and we discover that, when l drops to 3nm and then keep it as constant, h expands from 1~100 nm. The change of the lateral strain with dimension h is shown in Figure 12. Now the two curves begin to deviate from each other clearly.

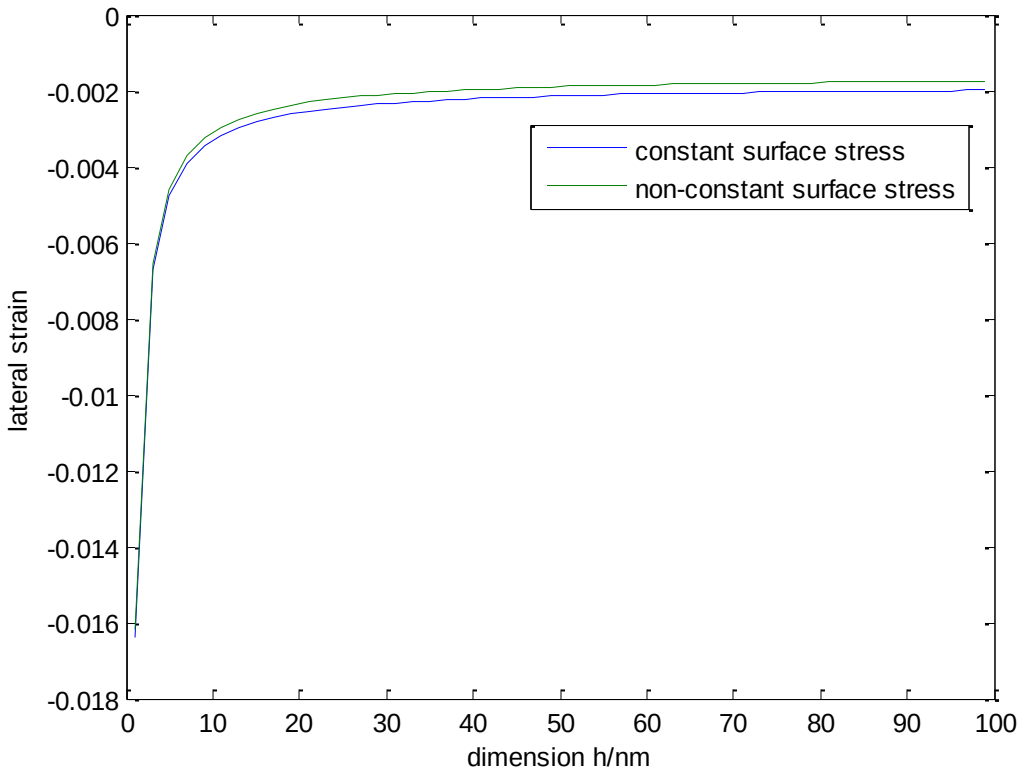

Figure 12: The change of the lateral strain with dimension h for surface effect(l=3nm)

To make it clear enough to see the difference of the effect of $\Gamma^{(2)}$ term on the lateral strain, we have to decrease dimension l from Figure 11 to Figure 12. We need to notice that the dimension is already below 10nm, which is very difficult to achieve in practical epitaxy. This shows that that $\Gamma^{(2)}$ term can have some influence on the lateral strain, but only when the length scale goes down to only several nanometers, and for some cases it can be neglected.

Summery and Future Work

In our work, we studied the stress and strain analysis of epitaxy in nano-scale materials, in which we seek a methodology to bridge the gap between continuum mechanical models and incorporate surface excess energy effects, which can be obtained by molecular dynamical simulations. In those chapters above, we made the description of the elastic behavior of the bulk material, covering the concepts of stress, strain, elastic energy and especially, the elastic constants. After that, we explained in details about the definitions of surface/interface excess energy and their characteristic property tensors. For both elastic constants and surface excess energy, our calculation principle is based on curve-fitting the parabola function between the total strain energy density and the strain.

After this, we analyzed the stress and strain state in nanoisland during the selective area growth of epitaxy. When the nanoisland is relaxed, the lattice structure becomes equilibrated, which means the total strain energy of system need to be minimized. Our framework of analysing the nanoisland begins with writing the system's strain energy in two parts: Bulk elastic energy contribution and surface excess energy contribution, and then we can apply the energy minimization principle to obtain the derivations of the strain state. Compared to other researcher's work, our model is based on continuum mechanics but also adopts the outcome from MD simulations. By combining these microscopic informations and those macroscopic observable properties, such as bulk elastic constants, we can provide a novel way of analyzing the stress and strain profile in epitaxy. The most important idea behind this approach is that, whenever we can obtain the elastic constants and surface property tensors from MD simulations, we can follow the same methodology to analyse the stress and strain in any epitaxy process, and quite a refined result can be obtained. This is the power of combining atomistic simulations and continuum method, which can take considerations of both the microscopic and macroscopic factors.

However, there is one regret of our work. In fact, we have also tried this approach to the epitaxy process of GaN(gallium nitride), which is also the highlight of semiconductor and optoelectronics industry. The result is not satisfactory since the calculated value of elastic constants deviate too much from experimental data. Our results of elastic constants C11, C12 are 489.1Gpa and 111.3Gpa, while they can be found to be around 390Gpa and 145Gpa on the authoritative "National compound semiconductor roadmap"website(http://www.onr.navy.mil/sci_tech/31/312/ncsr/materials/sic.asp).

The biggest problem is that there is no available proper interatomic potential for this kind of material to simulate its property yet. This is also the reason that we stressed the importance of interatomic potentials for atomistic simulations at the very beginning.

In fact, our analysis of nanoisland is still quite a simplified case. In practical epitaxy applications, the strain distribution could be quite complex, which may vary for each point. On the other hand, considering the possibilities of all kinds of nanoisland shapes in epitaxy, the surface energy term could be extremely complicated. In the further study, it would be better to consider a general strain field(nonhomogeneous, and shear effect also exists) with finite element method, and surface excess energy is also included in this framework. In that case, we can also take consideration of a general anisotropic material. That means we need to obtain all elastic constants and all surface property tensors from MD simulations, then put them into the finite element method calculation, and hopefully we can get a better strain profile.

REFERENCES

[1] Z. I. Alferov, Reviews of Modern Physics 73(2001): 767.

[2] E. J. Thrush, etc., Mater. Sci. Eng. B 21(1993): 130.

[3] T. Takiguchi, etc., J. Cryst. Growth 170(1997): 705.

[4] T. Sasaki, etc., IEICE Trans. Electron. E80-C(1997): 654.

[5] K. F. Jensen, Elsevier 3A(1994): 541.

[6] G. H. Gilmer, Elsevier 1A(1993): 583.

[7] M. M. IslamRaja, etc., J. Appl. Phys. 70(1991): 7137.

[8] A. Dollet, Surface and Coatings Technology 177 –178(2004): 245.

[9] K. Ohno, etc., Computational Materials Science, Springer, Berlin, 1999.

[10] D. Raabe, Computational Materials Science, Wiley–VCH, Weinheim, 1998.

[11] S. J. Plimpton, J. Comp. Phys. 117(1995): 1.

[12] Daw, etc., Phys. Rev. Lett. 50(1983): 1285.

[13] J. W. Martin, Journal of Physics C 8(1975): 2837.

[14] R. Shuttleworth, Proceedings of the Royal Society of London A 63(1950): 444.

[15] C. Herring, Journal of Applied Physics 21(1950): 437.

[16] W. W. Mullins, Journal of Applied Physics 30(1959): 77.

[17] P. Sharma, and S. Ganti, Journal of Materials Research 18(8): 1823.

[18] A. F. Andreev, and Y. A. Kosevich, Soviet Physics-JETP 54(1981): 761..

[19] R. Dingreville, PhD thesis. Georgia Institute of Technology(2007).

[20] R. Dingreville, and J.Qu, Computational Materials Science 46(2009): 83.

[21] L. Capolungo, etc., International Journal of Plasticity 21(1): 67.

[22] Y. Hiki, and A. V. Granato, Physical Review 144(2): 411.

[23] S. M. Foiles, etc., Physical Review B 33(12): 7983.

[24] P. Gumbsch, and M. S. Daw, Physical Review B 44(8): 3934.

[25] G. J. Ackland, etc., Philosophical Magazine A 56(6): 735.

[26] S. Nakamura, etc., Appl. Phys. Lett. 72(1998): 211.

[27] J. H. Moths, Dislocations in Solids, 1979.

[28] J. A. Venables, and P. S. Schates-Retchziman, J. Phys. (Paris) Colloq. 4(38): 116.

[29] A. D. Novaco, and J. P. McTaqgue, Phys. Rev. Lett. 38 (1977): 1286.

[30] D. A. Huse, Phys. Rev. B 29(1984): 6985.

[31] D. B. Pengra, etc., Surf. Sci. 245(1991): 125.

[32] R. Kern, and P. Muller, Surface Science 392(1997): 103.

[33] F.K. Legoues, etc., Phys. Rev. B 42(1990): 11690.